Macromolecular Bioscience
www.mbs-journal.de

Synthesis and Application of Low Molecular Weight PEI-Based Copolymers for siRNA Delivery with Smart Polymer Blends

*Yao Jin, Friederike Adams, Judith Möller, Lorenz Isert, Christoph M. Zimmermann, David Keul, and Olivia M. Merkel**

Polyethylenimine (PEI) is a commonly used cationic polymer for small-interfering RNA (siRNA) delivery due to its high transfection efficiency at low commercial cost. However, high molecular weight PEI is cytotoxic and thus, its practical application is limited. In this study, different formulations of low molecular weight PEI (LMW-PEI) based copolymers polyethylenimine-*g*-polycaprolactone (PEI–PCL) (800 Da–40 kDa) and PEI–PCL–PEI (5–5–5 kDa) blended with or without polyethylene glycol-*b*-polycaprolactone (PEG–PCL) (5 kDa-4 kDa) are investigated to prepare nanoparticles via nanoprecipitation using a solvent displacement method with sizes ≈100 nm. PEG–PCL can stabilize the nanoparticles, improve their biocompatibility, and extend their circulation time in vivo. The nanoparticles composed of PEI–PCL–PEI and PEG–PCL show higher siRNA encapsulation efficiency than PEI–PCL/PEG–PCL based nanoparticles at low N/P ratios, higher cellular uptake, and a gene silencing efficiency of ≈40% as a result of the higher molecular weight PEI blocks. These results suggest that the PEI–PCL–PEI/PEG–PCL nanoparticle system could be a promising vehicle for siRNA delivery at minimal synthetic effort.

1. Introduction

After RNA interference (RNAi) was discovered over 20 years ago,[1] the field of RNAi-based therapeutics is now growing rapidly. The first siRNA-based drug patisiran (Onpattro is a trademark of Alnylam Pharmaceuticals) was approved by the U.S. FDA in 2018 for polyneuropathy of hereditary transthyretin-mediated amyloidosis, and givosiran (Givlaari is a trademark of Alnylam Pharmaceuticals) was approved in 2019 for acute hepatic porphyria.[2,3] In 2020, lumasiran (Oxlumo is a trademark of Alnylam Pharmaceuticals) was approved for the treatment of primary hyperoxaluria type 1.[4] In 2021, inclisiran (Leqvio is a trademark of Novartis) was approved and the latest approved siRNA agent is vutrisiran (Amvuttra is a trademark of Alnylam Pharmaceuticals). Despite this success, the approved siRNA-based drugs target the liver, and other organs cannot be addressed with the one approved delivery system. The approval of siRNA-based drugs and the shortcomings of current siRNA delivery strategies fostered a new interest from industrial and academic groups in RNAi therapeutics.[3] However, the delivery of siRNA, which is a double-stranded siRNA with 21–25 nucleotides and can induce RNAi, remains a challenge. As siRNA molecules are hydrophilic, anionic macromolecules, they cannot

Y. Jin, F. Adams[+], J. Möller, L. Isert, C. M. Zimmermann, D. Keul, O. M. Merkel
Department of Pharmacy
Ludwig-Maximilians-University Munich
Pharmaceutical Technology and Biopharmaceutics
Butenandtstr. 5–13, 81377 Munich, Germany
E-mail: olivia.merkel@lmu.de

The ORCID identification number(s) for the author(s) of this article can be found under https://doi.org/10.1002/mabi.202200409

[+]Present address: Chair of Macromolecular Materials and Fiber Chemistry, Institute of Polymer Chemistry, University of Stuttgart, Pfaffenwaldring 55, 70569 Stuttgart, Germany

DOI: 10.1002/mabi.202200409

F. Adams[+]
Department of Ophthalmology
University Eye Hospital Tübingen
Center for Ophthalmology
Elfriede-Aulhorn-Strasse 7, 72076 Tübingen, Germany
C. M. Zimmermann
Department for Chemistry
University of Bern
Biochemistry and Pharmacy
Freiestrasse 3, Bern 3012, Switzerland

cross cell membranes by passive diffusion for efficient cellular uptake; also, due to enzymatic degradation, and its fast renal clearance, the half-life of naked siRNA in blood circulation is very short.[5]

Among the vast family of non-viral nucleic acid delivery systems, polyethylenimine (PEI) and its derivatives have taken a prominent position due to their high encapsulation efficiency at low commercial cost.[6] However, the transfection efficiency and cytotoxicity of PEI are strongly dependent on the molecular weight.[7] PEI with high molecular weight (HMW-PEI), such as the commonly used branched PEI with a molecular weight of 25 kDa, exhibits both higher transfection efficiency and higher cytotoxicity than smaller PEIs.[8,9] In addition, high molecular weight PEI may accumulate during in vivo application, since there is no degradation pathway or a mechanism of excretion known for such molecules.[8] Low molecular weight PEI (LMW-PEI, <22 kDa) shows low cytotoxicity and can also be eliminated from systemic circulation through the kidneys.[10] However, the lower molecular weight also causes low transfection efficiency due to weak nucleic acid binding abilities and insufficient protection from nucleases.[7] To circumvent the low transfection efficiency of LMW-PEI, researchers have adopted various strategies, for example, crosslinking LMW-PEI to form biodegradable HMW-PEI,[11,12] modifying with polyethylene glycol (PEG), targeting peptides, amino acids,[13] and hydrophobic groups.[14] For example, Karimov et al. combined the strategies of disulfide cross-linking and the amino acid tyrosine- modification of low molecular weight PEI to enhance its transfection efficacy and biocompatibility.[15] In particular, hydrophobic group conjugation to LMW-PEI has been proven to be an effective strategy to improve nucleic acid delivery, which may be due to the improved cellular uptake, endosomal escape, and the unpacking of polyplexes intracellularly.[16–18] For example, Zheng et al. conjugated lipoic acid to PEI (Mw 1800 Da) and increased the transfection efficiency in 293T cells and Hela cells.[16]

Amphiphilic polymer structures containing polycaprolactone (PCL) as hydrophobic segments grafted onto PEI could in principle form micelles exhibiting a core–corona structure with improved colloidal stability in aqueous dispersion and biological fluids. Also, the micelle-like architecture could potentially promote the transmembrane transport, thus enhancing the transfection efficiency.[19,20] Moreover, the core–corona architecture could offer the possibility of multi-functionality whereby the co-delivery of siRNA in the corona by electrostatic interaction and hydrophobic chemicals (e.g., quantum dots, paclitaxel) in the core due to the hydrophobic interaction could be achieved.[21]

The main goal of this study is to develop an efficient and safe siRNA delivery system based on LMW-PEI. We compared LMW-PEI-based copolymers polyethylenimine-*g*-polycaprolactone (PEI–PCL) (800 Da–40 kDa) and PEI–PCL–PEI (5–5–5 kDa) with varying amounts of cationic and hydrophobic ratios and block structures and separately blended each copolymer with polyethylene glycol-*b*-polycaprolactone (PEG–PCL) (5–4 kDa) to prepare nanoparticles via nanoprecipitation (solvent displacement). PEG–PCL functions as a stabilizer in the nanoparticles, where the PEG section can shield the positive charge of PEI to improve the nanoparticles' biocompatibility; PEG can also counteract protein absorption while maintaining suspension stability and extending the circulation time in blood.[22] Compared with the triblock copolymer PEI–PCL-PEG, the blending strategy allows us to alter the amount of PEG easily to find a balance between biocompatibility and transfection efficiency of the nanoparticles. Besides, ligand-modified PEG–PCL can be used in the next step, and the smart blending allows for easy adjustment of the amount of ligand to achieve efficient targeted delivery. In this paper, three methods were compared to optimize the preparation of nanoparticles for optimized size and zeta potential of the nanoparticles, siRNA encapsulation efficiency, cellular uptake, and GFP knockdown efficiency.

2. Results and Discussion

2.1. Size and Zeta Potential of NPs–siRNA Complexes

The commercially available polymer PEI–PCL (800 Da–40 kDa) was initially used to prepare nanoparticles. Because of the poor solubility of this polymer in water due to a high hydrophobic polymer ratio, the NPs–siRNA complexes were prepared by nanoprecipitation methods. The typical procedure for nanoprecipitation is to dissolve the polymers in water-miscible organic solvents (organic phase) and to add the organic phase to a nonsolvent of polymer (aqueous phase). The PEI–PCL is not soluble in acetone or ethanol but soluble in tetrahydrofuran (THF). Therefore, THF was chosen for all experiments with PEI–PCL and three different methods were evaluated for the formation of NPs–siRNA at various N/P ratios. Method 1 is a common method, where the blank NPs are prepared first and then loaded with siRNA; for method 2, the siRNA was dissolved in HEPES buffer and interacted with polymers during the process of nanoparticle formation; for method 3, siRNA and polymers were incubated first for efficient binding and then added dropwise to HEPES buffer (**Scheme 1**).

As shown in **Figure 1**, the NPs–siRNA prepared by methods 1 and 2, in general, had smaller sizes (≈100 nm) than the ones prepared by method 3. However, the sizes of NPs–siRNA prepared with method 1 at N/P 7 and 10 were large. It was hypothesized that the net charges of the nanoparticles were not sufficient to stabilize the nanoparticles as reflected by the neutral zeta potential. The large sizes of NPs–siRNA obtained with method 2 at N/P 6 can also be explained by aggregation and insufficient siRNA encapsulation due to the same reasons.

Nanoprecipitation (solvent displacement) is one of the most commonly used methods for preparing biodegradable submicron particles.[23] Different mechanisms have been proposed to explain particle formation of the solvent displacement technique. Vitale and Katz proposed the "ouzo effect" in 2003.[24] On mixing with water, the oil becomes supersaturated, which results in the nucleation of oil droplets. Oil immediately begins to diffuse to the nearby droplets, until the supersaturation decreases and no further nucleation occurs.[25]

Various parameters can influence nanoprecipitation. For instance, the stirring rate can influence the size and entrapment efficiency of the nanoparticles. A low stirring speed rate leads to high drug entrapment efficiency,[26] while a high stirring speed can produce nanoparticles of smaller size.[27] The size of the nanoparticles is also related to the polymer concentration in the organic phase, where lower concentrations could produce smaller nanoparticles.[28] Besides, the system

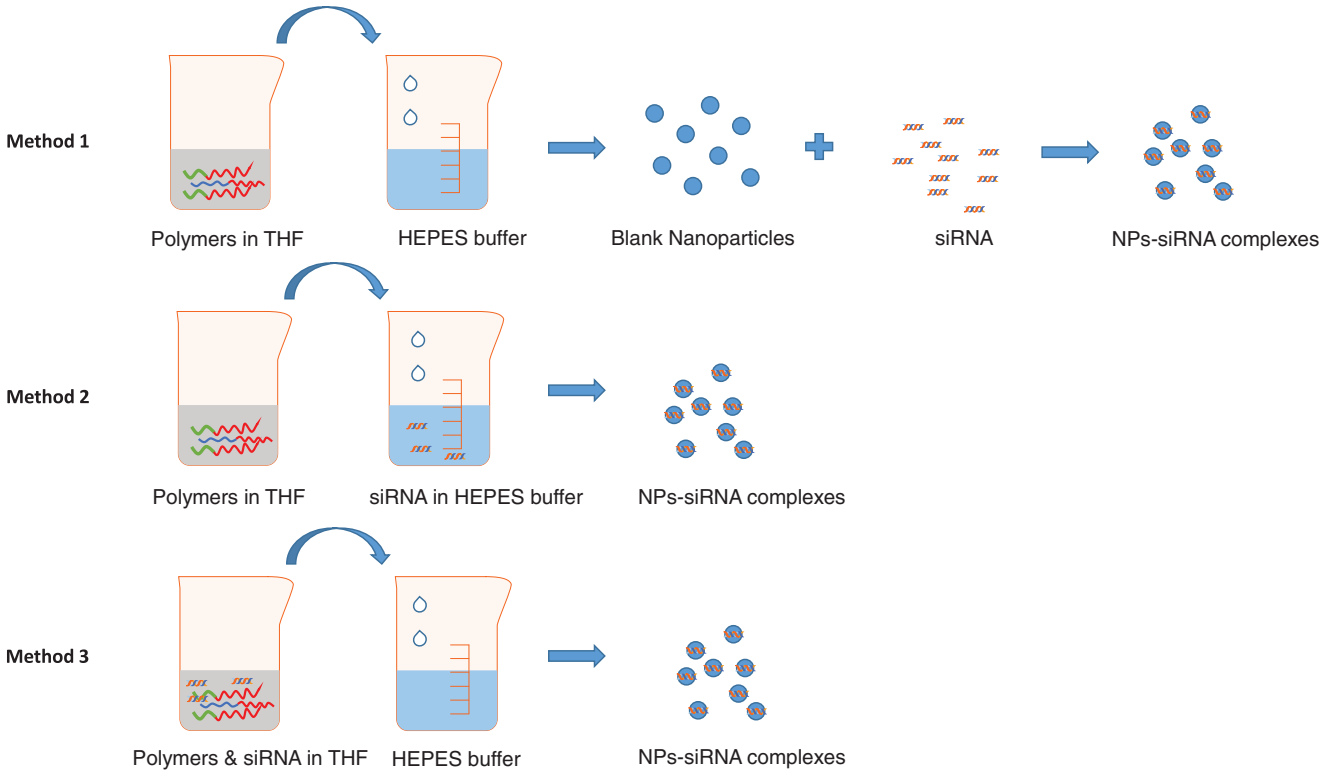

Scheme 1. Schematic illustration of NPs–siRNA complexes preparation methods 1–3.

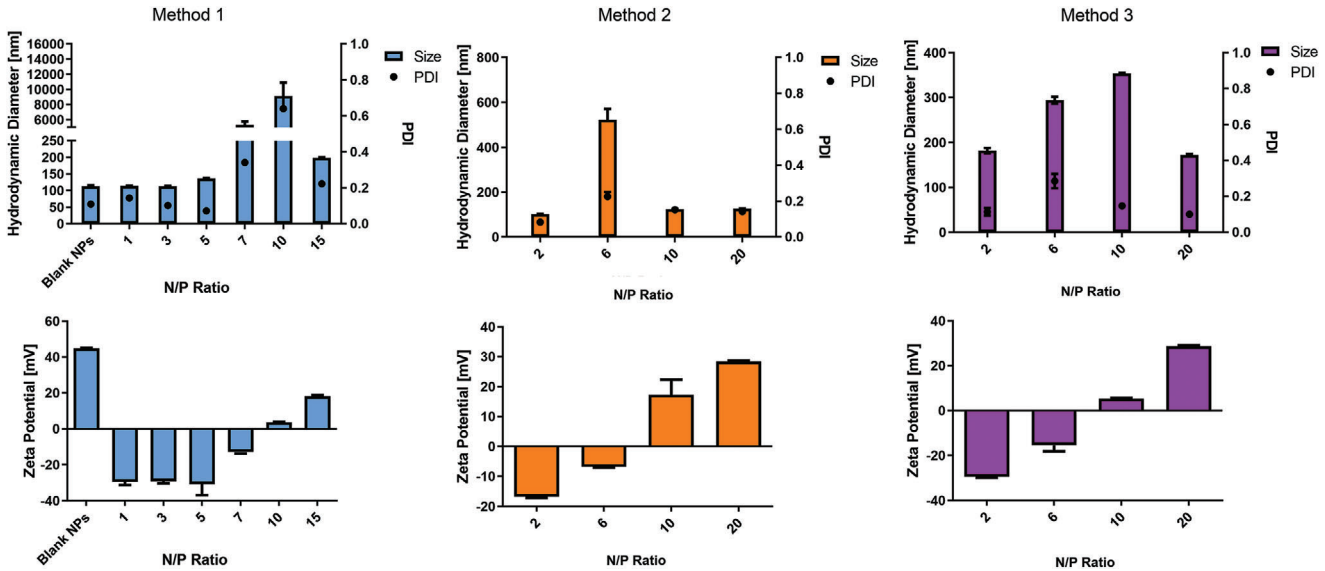

Figure 1. Hydrodynamic diameter (Size), polydispersity index (PDI), and zeta potential of NPs–siRNA prepared by methods 1 (blue), 2 (orange), and 3 (purple).

temperature and organic phase addition method can also influence the characteristics of the nanoparticles.[23] The organic phase can be added to the aqueous phase dropwise[29] or rapidly dispersed[30] or added at a constant speed.[31] Here, we added the organic phase (THF solution) dropwise which is a commonly used method.

The amphiphilic diblock copolymer PEG–PCL is rationally used as a stabilizer in this experiment. The aqueous suspensions of hydrophobic solute NPs are non-equilibrium systems, and the high interfacial surface area renders such systems prone to aggregation. Thus a stabilizer is necessary unless the surface is charged, or modified through adsorption of ionic surfactants or

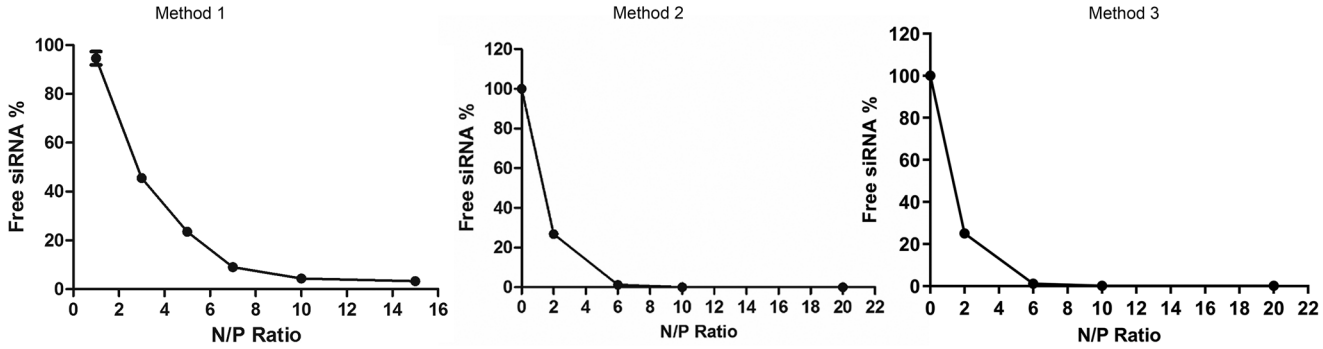

Figure 2. siRNA encapsulation efficiency of PEI–PCL/PEG–PCL nanoparticles prepared by methods 1, 2, and 3 measured by SYBR gold assay. The fluorescence of free siRNA was set as 100% fluorescence value. Data points indicate mean ± SD, $n = 3$.

polymers.[28,32] PEG–PCL offers several advantages: during NPs formation, it can arrest solute particle growth and provide stabilization before aggregation; PEG can prolong the circulation time in vivo; as a diblock copolymer, PEG–PCL has lower critical micelle concentration (CMC) than small-molecule surfactants, which enhances the stability of nanoparticles and offers longer protection from opsonization in vivo.[28,32]

2.2. SYBR Gold Assay of PEI–PCL/PEG–PCL Nanoparticles

The siRNA encapsulation efficiency of the nanoparticles prepared by methods 1, 2, and 3 were all determined by SYBR gold assays. In this assay, free or unbound siRNA is accessible to the intercalating dye SYBR gold, and is quantified based on the fluorescence emitted.[33] The data is reported as the ratio of the formulation's fluorescence to free siRNA. This measurable fluorescence may stem from siRNA either not encapsulated by nanoparticles or surface-bound and still accessible to SYBR gold. As shown in **Figure 2**, the nanoparticles prepared by method 1 where siRNA is added to pre-formed particles cannot encapsulate siRNA quantitatively even at N/P 15, while the nanoparticles prepared by methods 2 and 3 can almost fully encapsulate the siRNA from N/P 6 on. The siRNA encapsulation efficiency of particles prepared by methods 2 and 3 is better than that of particles prepared by method 1. This observation can be explained by the siRNA more adequately interacting with PEI–PCL in a small volume and before the NPs are formed. The siRNA encapsulation trends of the particles prepared with the three different methods are corresponding to the zeta potential of the nanoparticles: when the siRNA was fully encapsulated, the zeta potential was positive possibly with PEI–PCL on the surface. However, when free siRNA was present on the surface, the zeta potential was negative. For NPs–siRNA prepared by method 2 and method 3 at N/P 6, still 1–2% of free siRNA was left, resulting in a negative zeta potential. Additionally, the PEG segment is also slightly negative in buffer, adding another explanation for the zeta potential of NPs–siRNA at N/P 6.

2.3. Cellular Uptake of PEI–PCL/PEG–PCL Nanoparticles

The cellular uptake of the NPs–siRNA complexes at various N/P ratios was determined by flow cytometry. As shown in **Figure 3**.

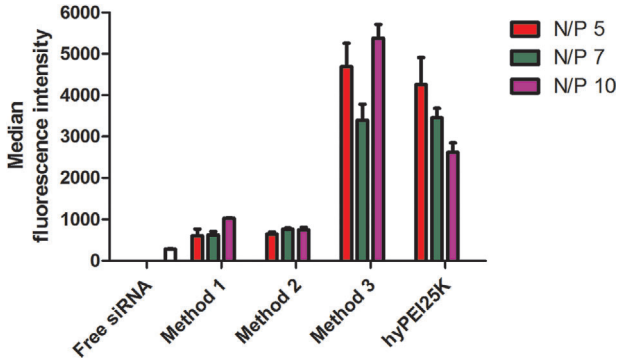

Figure 3. Cellular uptake of NPs loaded with AF488-siRNA prepared by method 1, method 2, and method 3 in H1299 cells as determined by flow cytometry (mean ± SD, $n = 3$).

The NPs–siRNA complexes prepared by method 3 showed the highest cellular uptake, which is assumed to result from the higher siRNA encapsulation efficiency of the latter nanoparticles. In method 3, the siRNA was incubated with PEI–PCL/PEG–PCL polymer in THF solution first, and the siRNA can bind with PEI–PCL during the incubation. It was also hypothesized that the siRNA can be encapsulated into the core of the nanoparticles when the polymer solution is added to the aqueous phase, thus efficiently protecting the siRNA from release. Similarly, Kly et al. first complexed pDNA with PCL-*b*-P2VP (poly(ϵ-caprolactone)-*block*-poly(2-vinyl pyridine)) in a dioxane/acetic acid/water mixture and then added PCL-PEG and extra water. The nanoparticles finally formed with a "polyplexes-in-hydrophobic-core" architecture.[34] Considering that the nanoparticle–siRNA complexes prepared by method 3 showed the highest cellular uptake, the GFP knockdown efficiency was determined, but did not achieve an efficient silencing effect (Figure S3, Supporting Information). This observation could be caused by limited release of siRNA from the nanoparticle. The nanoparticles prepared by method 2 showed siRNA encapsulation efficiency comparable with method 3 but much lower cellular uptake, which could be attributed to the low binding capacity of PEI (800 Da) and low stability. To prove our assumption, heparin competition assays were performed.

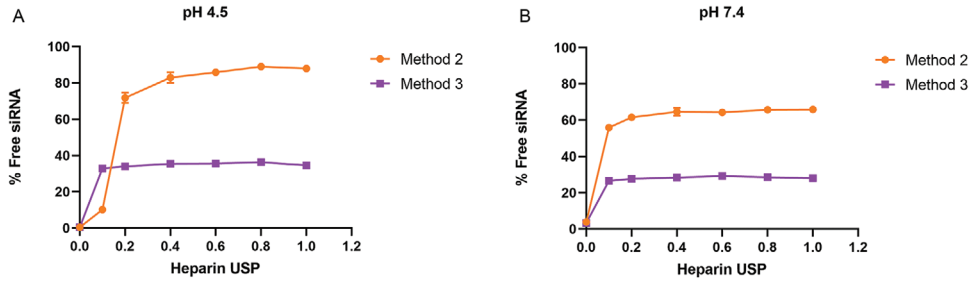

Figure 4. Release profiles of siRNA from NPs–siRNA complexes (N/P = 10) prepared by methods 2 and 3 in presence of heparin at A) pH 4.5 and B) pH 7.4. Results are given as mean normalized fluorescence (mean ± SD, $n = 3$).

2.4. Heparin Competition Assay of PEI–PCL/PEG–PCL Nanoparticles

To evaluate the stability of the NPs–siRNA complexes and have a deeper understanding of the different behavior of the nanoparticles prepared by different methods, heparin competition assays were evaluated. For nonviral vectors, complex stability is important and is influenced by the presence of competing anions in the cell membrane or serum.[35–37] The heparin competition assay was performed in the neutral (pH 7.4) and acidic (pH 4.5) buffer to mimic the environment of cytoplasm and endo/lysosomes, respectively. The nanoparticles prepared by method 2 and method 3 were selected because of their relatively better siRNA encapsulation efficiency and higher cellular uptake. As shown in **Figure 4**, the stability of all NPs–siRNA complexes decreased with increasing heparin concentration, and siRNA was released due to the competition with heparin polyanions. The release of siRNA at pH 4.5 was a bit higher than at pH 7.4, which could be due to the further protonation of PEI and the repulsion of the PEI molecules which loosens the previously compact polyplex and makes the siRNA more accessible to heparin, thus promoting the siRNA release.[38,39] In case of the nanoparticles prepared by method 3, the siRNA was also physically entrapped inside the nanoparticles, so the heparin did not reach these siRNA, resulting in an overall low RNA release. Therefore, these nanoparticles were more stable in the presence of competing polyanions such as negatively charged proteins in serum, which may explain the higher cellular uptake of these nanoparticles. While polyplexes on the one hand need to be stable to protect the siRNA from the competition with other polyanions and degradation from enzymes, on the other hand, the siRNA has to be released to the cytoplasm to induce RNAi. If the siRNA molecules are bound too tightly in the particles with too little release, the gene silencing efficiency of the nanoparticles can be limited as well. Finding a balance between the nanoparticles' stability and release property is still a major hurdle in the field of non-viral RNA vectors.

Taking the results of the SYBR gold assays, cellular uptake and heparin assays together, the binding capacity of the nanoparticles seems important. Optimizing the formulation technique of the nanoparticles improved the cellular uptake. However, the formed NPs are still not efficient for gene silencing. Therefore, we decided to synthesize a polymer using an intermediate molecular weight of PEI (5 kDa).

2.5. Synthesis of PEI5K–PCL5K–PEI5K

Polyethylenimine (branched PEI, 5 kDa) was conjugated to polycaprolactone-diacrylate (PCL-diacrylate, 5 kDa) via Michael addition reaction, and the unconjugated polymer was removed by dialysis. As shown in the ^{1}H NMR spectra in Figure S1, Supporting Information, the peaks ≈5.83, ≈6.12, and ≈6.36 ppm belonging to the acrylate group of PCL-diacrylate disappeared in the spectrum of PEI–PCL–PEI, which confirms successful conjugation of PEI and PCL-diacrylate. The peaks between 2.5 and 2.9 ppm belong to PEI, the peaks at 1.38, 1.64, 3.30, and 4.06 ppm belong to PCL.

2.6. Characterization of PEI–PCL–PEI/PEG–PCL Nanoparticles

The hydrodynamic diameter (size) and zeta potential of the PEI–PCL–PEI/PEG–PCL nanoparticles were characterized by dynamic light scattering (DLS) and laser doppler anemometry (LDA). As shown in **Figure 5**, increasing amounts of PEG–PCL were used in different batches. The sizes of the nanoparticles were all ≈60 nm: the nanoparticles without PEG–PCL (PPP) were 63.69 nm, and the nanoparticles with 2, 4, and 8 µL PEG–PCL (5 mg mL^{-1}) were all ≈56 nm small. Slight differences reflect batch-to-batch variability. The amount of PEG–PCL did not have a visible influence on the size of the nanoparticles. There is a slight difference from batch to batch, which might be due to the speed of adding organic solvents or the variation of room temperature. However, the sizes of the nanoparticle were all in the range of 50–100 nm, which is not expected to lead to big differences regarding the in vitro performance.[40] The zeta potentials of all the nanoparticles without loading siRNA were ≈40 mV. When loaded with siRNA at different N/P ratios, the sizes of the NPs–siRNA complexes differed depending on the N/P ratio, and ranged from 61.1 (PPP/PP NPs–siRNA N/P 3) to 108.7 nm (PPP NPs–siRNA N/P 1). For PEI5K–PCL5K–PEI5K, we assume that the higher molecular weight of PEI is sufficient enough to encapsulate siRNA. Therefore, we prepared blank nanoparticles first and loaded them with siRNA afterward (method 1). Acetone was used instead of THF because of its lower boiling point for evaporation and removal. Also, acetone is better tolerated by cells and tissues.[41] Indeed, acetone was also initially chosen for the polymer PEI–PCL (800–40 kDa), however, due to its insolubility in acetone, THF was used as an alternative. Not surprisingly, we

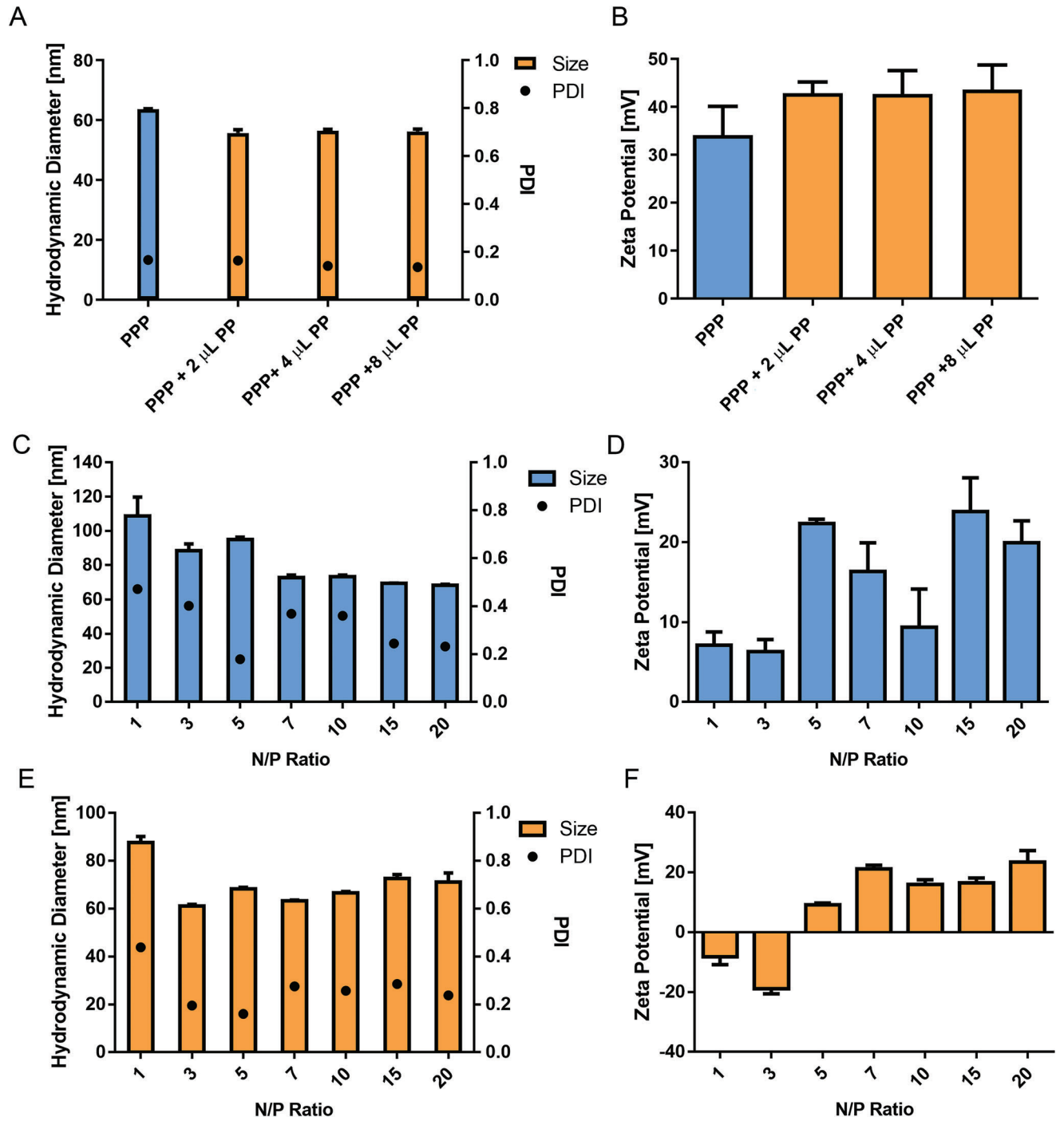

Figure 5. A,B) Size and zeta potential of PEI–PCL–PEI/PEG–PCL blank nanoparticles with different amounts of PEG–PCL. C,D) Size and zeta potential of PEI–PCL–PEI NPs–siRNA complexes. E,F) Size and zeta potential of PEI–PCL–PEI/PEG–PCL NPs–siRNA complexes (2 μL PEG–PCL). PPP: PEI5K–PCL5K–PEI5K (5 mg mL^{-1}, 200 μL), PP: PEG–PCL (5 mg mL^{-1}).

did observe cytotoxicity with THF, which cannot be eliminated by overnight evaporating under fume hood, in vacuo or dialysis, but can only be removed by freeze-drying (Figure S2, Supporting Information). When distilled water was used for the preparation of PEI–PCL based nanoparticles, the sizes of the nanoparticles were not reproducible. Hence, 10 mM HEPES was used for the PEI–PCL based nanoparticles, while for PEI5K–PCL5K–PEI5K based nanoparticles we did not have this problem using distilled water. This could be due to the different net charge of the PEI segments in the polymers leading to different colloidal stability. Methods 2 and 3 were not used with PEI–PCL–PEI, because on one hand, the content of PEI of the triblock copolymer was much

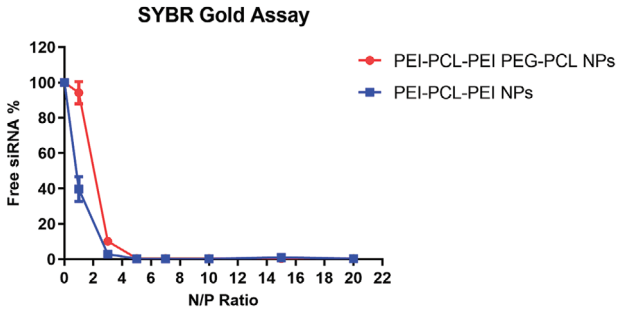

Figure 6. siRNA encapsulation efficiency of PEI–PCL–PEI NPs and PEI–PCL–PEI/PEG–PCL nanoparticles measured by SYBR gold assay at increasing N/P ratios. The fluorescence of free siRNA was set as 100%, mean ± SD, $n = 3$.

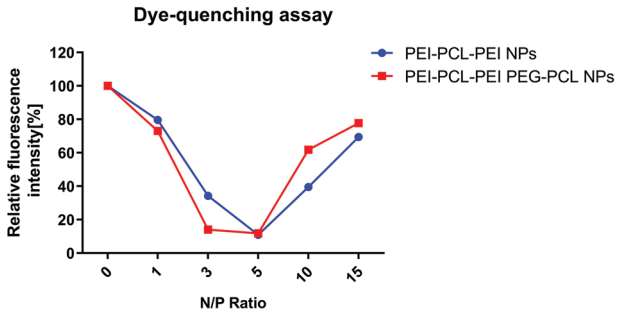

Figure 7. Dye quenching assay. The fluorescence of Cy5-labeled siRNA molecules is quenched by each other in a "multimolecular complex" due to close spatial proximity. Both curves have a minimum fluorescence at N/P = 5, after which the fluorescence increases again due to a decreased number of siRNA molecules per nanoparticle.

higher than that of PEI–PCL. Additionally, to prepare nanoparticles with method 2 and method 3, a lot of siRNA was necessary, and the produced micelleplexes are unstable and uneconomical for storage. For method 1, the blank NPs can be simply stored at 4 °C. On the other hand, for method 2 and 3, there might be possible degradation of siRNA during the solvent evaporation process over 3 h. In fact, the PEI–PCL/PEG–PCL nanoparticles prepared by method 3, did not mediate significant GFP knockdown (Figure S3, Supporting Information) although they showed a relatively high cellular uptake. One possible explanation could be degradation of siRNA during preparation or storage, or a limited release of siRNA, of course.

2.7. siRNA Encapsulation Efficiency of the PEI–PCL–PEI/PEG–PCL Nanoparticles

The siRNA encapsulation efficiency of the PEI–PCL–PEI nanoparticles with and without PEG–PCL was determined by SYBR gold assay. As shown in **Figure 6**, the NPs with 2 µL PEG–PCL have lower encapsulation efficiency at N/P 1 and 3, which could be due to steric hindrance of PEG–PCL. However, this hindrance effect was compensated for at higher N/P ratios. Both nanoparticle types (PEI–PCL–PEI NPs and PEI–PCL–PEI/PEG–PCL NPs) can quantitatively encapsulate siRNA from N/P 5 on. Compared with the nanoparticles prepared from PEI–PCL (800 Da–40 kDa) (Figure 2, method 1) which cannot quantitatively encapsulate siRNA even at N/P 15, the siRNA encapsulation efficiency of this PEI5K–PCL5K–PEI5K based NPs is highly efficient.

2.8. Dye Quenching Assay

A dye quenching assay was also applied to investigate the binding behavior of nucleic acids by PEI–PCL–PEI nanoparticles with and without PEG–PCL. The Cy5-labeled siRNA is encapsulated in the polyplexes and when the spatial proximity of the Cy5-siRNA molecules are close enough, the fluorescence of Cy5 will be quenched by each other.[42] As shown in **Figure 7**, the relative fluorescence intensity was lowest at N/P 5, which means that the highest number of siRNA molecules was encapsulated per particle at this N/P ratio. This result corresponds to the SYBR gold assay result where siRNA was quantitatively encapsulated from N/P of 5 or higher. It was described earlier that with an increase of the N/P ratio beyond this point the siRNA molecules are distributed to more nanoparticles. Thus the amount of siRNA in each particle is less leading to a decreased quenching effect and increased relative fluorescence intensity.[42]

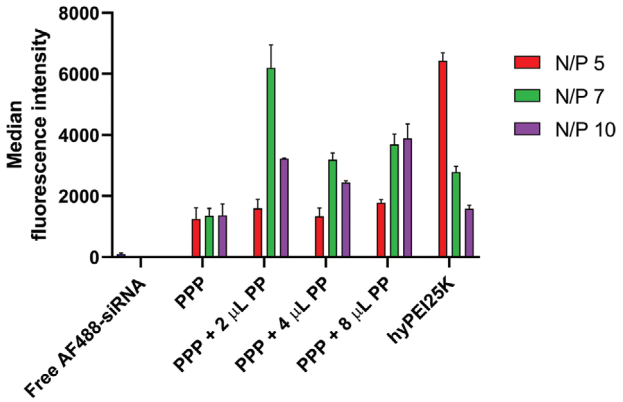

Figure 8. Cellular uptake of PEI–PCL–PEI/PEG–PCL NPs loaded with AF488-siRNA in H1299 cells quantified by flow cytometry and corrected by the autofluorescence of untreated cells. PPP: PEI5K-PCL5-PEI5K, 5 mg mL^{-1}, 200 µL. PP: PEG–PCL, 5 mg mL^{-1}.

2.9. Cellular Uptake of PEI–PCL–PEI/PEG–PCL Nanoparticles

The cellular uptake of PEI–PCL–PEI/PEG–PCL nanoparticles loaded with AF488-siRNA was measured by flow cytometry. As shown in **Figure 8**, the cellular uptake of PEI–PCL–PEI (PPP) nanoparticles without any PEG–PCL showed relatively low cellular uptake. The formulation PEI–PCL–PEI (5 mg mL^{-1}, 200 µL) with PEG–PCL (5 mg mL^{-1}, 2 µL) showed the highest cellular uptake at N/P 7 which is even higher than the uptake mediated by hyperbranched PEI with a molecular of 25 kDa (hyPEI25K, N/P 7). Interestingly, the NPs–siRNA complexes with 4 µL PEG–PCL and 8 µL also showed a lower cellular uptake than the formulations with 2 µL PEG–PCL. For the nanoparticles with various amounts of PEG–PCL, the cellular uptake at N/P 10 is a bit lower, which could be due to possible cytotoxicity. The nanoparticles with PEG–PCL showed higher cellular uptake which was

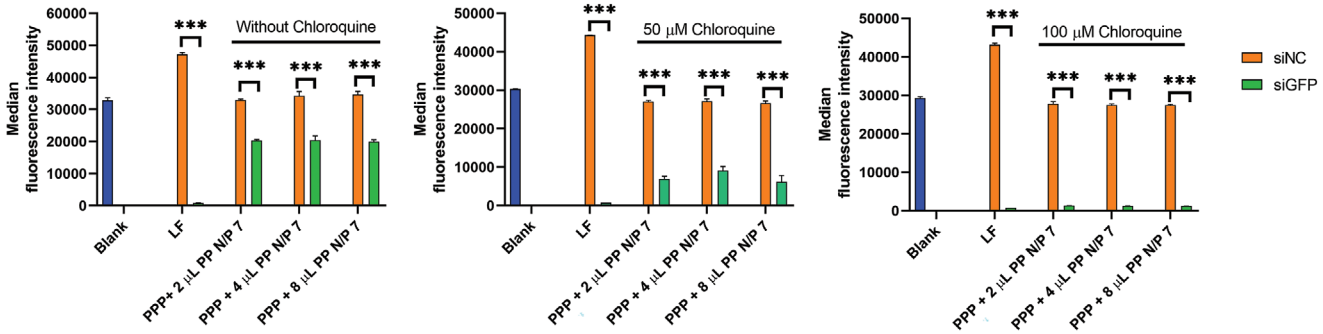

Figure 9. Green fluorescent protein (GFP) knockdown within a H1299 cell line stably expressing eGFP (H1299/eGFP cells). LF: Lipofectamine 2000, PPP:PEI5K–PCL5K–PEI5K, PP:PEG–PCL, siNC:negative control siRNA, siGFP:siRNA against eGFP (mean ± SD, $n = 3$, one-way ANOVA, $^{***}p < 0.001$).

hypothesized to be a result of PEG mediating serum stability in a serum-containing cell culture medium.[22] However, too much PEG is known to shield the positive charge of PEI, which in principle could improve cellular bioavailability but also weakens the interaction of the nanoparticles with the cell membrane, thus leading to a decreased cellular uptake.[43] We also found that PEI–PCL–PEI should be freshly synthesized, and the solubility of PEI–PCL–PEI in acetone decreased after storage at −20 °C, which could be due to PCL aggregation or partial degradation of PCL as well as PEI gelling.

2.10. GFP Knockdown of PEI–PCL–PEI/PEG–PCL Nanoparticles

To evaluate the gene silencing efficiency of the nanoparticles on the protein level, we evaluated knockdown of enhanced green fluorescent protein knockdown (eGFP) in stably expressing cells after transfection with PEI–PCL–PEI nanoparticles containing different amounts of PEG–PCL nanoparticles at N/P 7. Only N/P 7 was chosen based on the cellular uptake results. As shown in **Figure 9**, the knockdown efficiency of PEI–PCL–PEI nanoparticles with 2, 4, and 8 μL PEG–PCL was 38.29%, 40.28%, and 42.34% respectively. Regardless of the formulations' different behavior in the cellular uptake experiment, their knockdown efficiency was comparable, which could be due to the limited endosomal escape ability of the nanoparticles. Endosomal escape is the biggest obstacle to intracellular siRNA delivery. Once internalized, the nanoparticles can be entrapped in endosome/lysosomes, thus leading to the degradation of siRNA.[44] It was hypothesized that only a small part of the internalized nanoparticles escaped successfully from the endosomes, thus resulting in similar GFP knockdown efficiency. Chloroquine is a small molecule which can promote endosomal escape, as shown in Figure 9. When 50 μM chloroquine was applied, the GFP knockdown efficiency increased from ≈40% to ≈70%, when 100 μM chloroquine was used, the knockdown efficiency increased to ≈95%, which confirmed the hypothesis of endosomal entrapment. Compared to working with the triblock copolymer PEI–PCL-PEG,[6] the amount of PEG–PCL in a blend system can be adjusted very easily. It should be noted that PEG on the one hand can improve biocompatibility, and on the hand may decrease the transfection efficiency of nanoparticles due to the shielding effect of positive charges.[43] Hence, flexible adjustment may allow for facile tuning of the formulation. Besides, when PEG is modified with targeting ligands, the amount of targeting ligands usually needs to be optimized to achieve high cellular uptake and accumulation in the targeted issue or organs.[45] Therefore, the blended PEG–PCL strategy allows more flexibility and ease of fine-tuning the formulation.

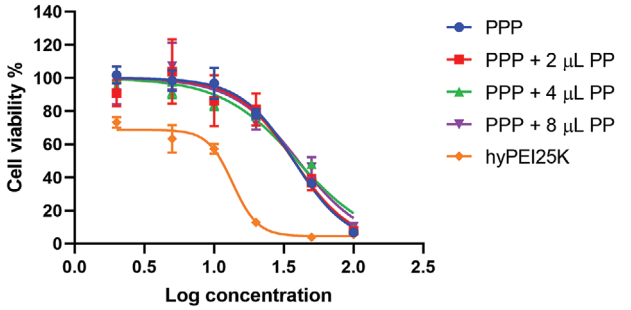

Figure 10. Cell viability of H1299 cells treated with PEI–PCL–PEI/PEG–PCL NPs determined by MTT assays. PPP:PEI5K–PCL5K–PEI5K, PP:PEG–PCL (mean ± SD, $n = 3$).

2.11. MTT assay of PEI–PCL–PEI/PEG–PCL based Nanoparticles

The cytotoxicity of PEI–PCL-PEG/PEG–PCL based nanoparticles (PPP/PP) was determined by MTT (thiazolyl blue tetrazolium bromide) assay.[46] As shown in **Figure 10**, all the nanoparticles showed higher cell biocompatibility than hyperbranched PEI. The IC50 of PPP is 37.43 μg mL^{-1}, PPP + 2 μL PP is 37.40 μg mL^{-1}, PPP + 4 μL PP is 39.44 μg mL^{-1}, and PPP + 8 μL PP is 40.13 μg mL^{-1}, and the IC50 hyperbranched PEI is 13.58 μg mL^{-1}. The application of PEG–PCL (PP) slightly improved the cell biocompatibility of the nanoparticles, which can be explained by a potential shielding effect of the positive charges of PEI by PEG–PCL.

3. Conclusion

In this project, we first utilized the commercially available PEI–PCL (800 Da–40 kDa) and PEG–PCL (5–4 kDa) to prepare nanoparticles. Based on the nanoprecipitation method, we developed three preparation methods and evaluated the siRNA encapsulation efficiency, size and zeta potential, and cellular uptake of

Table 1. Sequences of siRNAs used in this study.

Name	Sense strand (5'–3')	Antisense strand (3'–5')
siNC	pCGUUAAUCGCGUAUAAUACGCGUat	CAGCAAUUAGCGCAUAUUAUGCGCAUAp
siGFP	pACCCUGAAGUUCAUCUGCACCACcg	ACUGGGACUUCAAGUAGACGGGUGGC

"p" represents a phosphate residue, lower case letters denote 2'-deoxyribonucleotides, capital letters express ribonucleotides, and underlined capital letters are 2'-O-methylribonucleotides.

the nanoparticles and found that the formulation technique had a strong impact on siRNA encapsulation and cellular siRNA uptake. However, we also found that the cellular uptake of PEI–PCL (800 Da–40 kDa) based nanoparticles was too low due to the low binding capacity and low stability of PEI–PCL in the presence of polyanions such as the proteins in serum. Increasing the molecular weight of PEI to 5 kDa significantly improved the siRNA encapsulation efficiency and cellular uptake. The final formulation PEI–PCL–PEI/PEG–PCL showed high cellular uptake comparable with hyperbranched PEI (25 kDa) and also achieved a significant gene silencing. These results suggested that the PEI–PCL–PEI/PEG–PCL nanoparticle system could be a promising vehicle for siRNA delivery.

4. Experimental Section

Materials: Branched PEI (M_n = 5 kDa, Lupasol G100 and Lupasol WF, M_n = 25 kDa, BASF, Germany), PEI–PCL (800 Da–40 kDa), PEG–PCL (5–4 kDa) and polycaprolactone-diacrylate (PCL-diacrylate, M_n = 5 kDa) were purchased from PolySciTech (Akina, Inc., USA). *N*,*N*-dimethylformamide (DMF), Chloroform-D (Eurisotop, Germany), siRNA targeting green fluorescent protein (siGFP) and scrambled non-specific control (siNC) were purchased from IDT (Integrated DNA Technologies, Inc., Leuven, Belgium) and the sequences are shown in **Table 1**. Further, polyethylenimine (branched PEI, M_n = 10 kDa), 2,4,6-trinitrobenzesulfonic acid (TNBS), RPMI-1640 medium, fetal bovine serum (FBS), Penicillin-Streptomycin (P/S), G418 disulfate salt solution, Dulbecco's phosphate buffered saline (PBS), 0.05% trypsin-EDTA solution, heparin sodium salt, HEPES (4-(2-hydroxyethyl)-1-piperazineethanesulfonic acid), and sodium acetate were purchased from Sigma-Aldrich (Taufkirchen, Germany). AlexaFluor 488 (AF488), and SYBR gold dye were obtained from Life Technologies (Darmstadt, Germany).

Preparation and Characterization of PEI–PCL/PEG–PCL Based Nanoparticles: The PEI–PCL/PEG–PCL nanoparticles were prepared by nanoprecipitation (solvent displacement method) and three methods were developed based on nanoprecipitation (Scheme 1).

Method 1: PEI–PCL (800 Da-40 kDa) and PEG–PCL (5 kDa-4 kDa) were dissolved in 400 µL THF with concentrations of 2 and 0.05 mg mL^{-1}. The polymer solution in THF was then added to 800 µL 10 mM HEPES buffer dropwise while stirring and was kept stirring at 350 rpm under a fume hood for 3 h to evaporate the THF. When the blank nanoparticles were prepared, nanoparticles were post-loaded with siRNA via simply incubation with the blank nanoparticles.

Method 2: A specific amount of siRNA calculated according to the desired N/P ratio was added to 800 µL 10 mM HEPES buffer. In parallel, 400 µL PEI–PCL/PEG–PCL THF solution was prepared as in method I and was added to the siRNA solution dropwise which was stirred at 350 rpm under a fume hood for 3 h.

Method 3: A specific amount of siRNA calculated according to the desired N/P ratio was mixed with 200 µL THF, and the PEI–PCL/PEG–PCL THF solution as prepared in method 1 in 200 µL THF was mixed with the siRNA THF solution and incubated at room temperature for 30 min. The siRNA/PEI–PCL/PEG–PCL was then added dropwise to 800 µL 10 mM HEPES buffer and stirred at 350 rpm under a fume hood for 3 h.

For the preparation of NPs–siRNA complexes, the amounts of PEI–PCL polymers were calculated according to the following equation:

$$m\,(PEI-PCL)\ (inpg) = 50pmol \times 52 \times N/P \times 43.1gmol^{-1}/3.08\% \quad (1)$$

where 52 is the number of nucleotides of the 25/27mer siRNA; N/P ratio is the molar ratio of the polymer's protonable amine groups (N) and the siRNA phosphate groups (P); 43.1 g mol^{-1} is the protonable unit of PEI; 3.08% is the PEI amount in PEI–PCL determined by TNBS assay as described in the following section.

The size and zeta potential of the blank nanoparticles (NPs) and siRNA-loaded nanoparticle complexes (NPs–siRNA) dispersed in 10 mM HEPES buffer were determined using the Nano ZS (Malvern Instruments Inc., Malvern, UK), for each measurement, measurements were taken in triplicate with 15 runs each and the mean value was reported.

SYBR Gold Assay of PEI–PCL/PEG–PCL Based Nanoparticles: SYBR gold assays were performed to determine the siRNA encapsulation efficiency of the NPs prepared as described above. In brief, the NPs–siRNA complexes were prepared at various N/P ratios via methods 1, 2, and 3. The NPs–siRNA was then added to black 96-well plates with 100 µL for each well in triplicates. Subsequently, 30 µL SYBR gold (4×) solution was added to each well and incubated in the dark at room temperature for 10 min. Free siRNA was used as a control for the 100% fluorescence value. The fluorescence was finally determined in a microplate reader (TECAN, Switzerland, excitation: 485/20 nm emission: 520/20 nm).

Cellular Uptake of PEI–PCL/PEG–PCL Based Nanoparticles: To determine the cellular uptake of NPs–siRNA, Alexa Fluor 488 labeled siRNA (AF488-siRNA) was used to prepare the NPs–siRNA. H1299 cells were seeded in 24-well plates (50 000 cells per well) and grown in the CO_2 incubator 24 h before use. Afterward, NPs–siRNA complexes (50 pmol AF488-siRNA per well) diluted in RPMI-1640 complete medium were added and incubated with the cells in the incubator for 24 h. Subsequently, the NPs–siRNA solution was discarded, and the cells were rinsed with PBS and detached with 0.05% Trypsin–EDTA. The detached cells were then washed with PBS another two times and analyzed via flow cytometry (Attune NxT Acoustic Focusing Cytometer, Thermo Fisher, Darmstadt, Germany) excited with a 488 nm laser and detected with a BL1 filter (530/30 nm).

Heparin Competition of PEI–PCL/PEG–PCL Based Nanoparticles: To estimate the different behaviors of the NPs–siRNA obtained by different preparation methods in cellular uptake and evaluate their stability in the presence of competing polyanions, heparin competition assays were performed. In brief, the NPs–siRNA (N/P 10) were prepared by methods 2 and 3 in HEPES buffer (pH 7.4) or sodium acetate buffer (pH 4.5), and free siRNA was used as negative control and set as 100% fluorescence value. The NPs–siRNA complexes and free siRNA were added to a 96 well plate (60 µL per well), and heparin solution with various concentrations from 0.1 to 1 USP per well was added (10 µL per well) and incubated at room temperature for 30 min. Subsequently, 4× SYBR gold solution was added (30 µL per well) and incubated in the dark for 10 min. Intercalation-caused fluorescence was determined with a microplate reader (TECAN, Switzerland, excitation: 485/20 nm emission: 520/20 nm).

Synthesis of PEI5K–PCL5K–PEI5K: PEI5K–PCL5K–PEI5K was synthesized as illustrated in **Scheme 2**. In brief, 100 mg PEI5K (branched PEI, M_n = 5 kDa) was dissolved in 5 mL DMF and stirred at 40 °C for about 10 min,

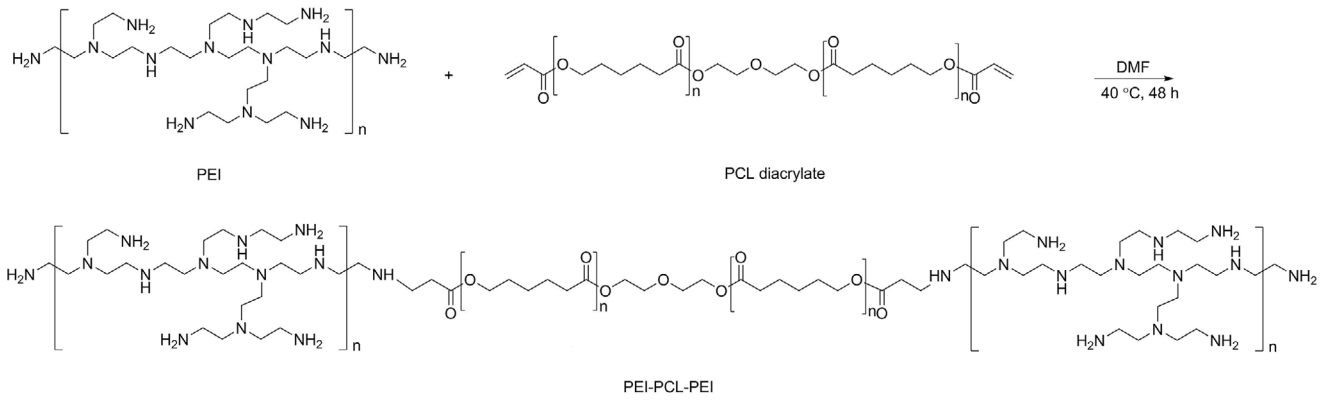

Scheme 2. Synthesis route of PEI5K–PCL5K–PEI5K.

then 50 mg polycaprolactone-diacrylate (PCL-diacrylate, M_n = 5 kDa) in 5 mL DMF was added dropwise to the PEI solution. After stirring at 40 °C for 48 h, the solution was transferred to a dialysis kit (MWCO 6 kDa, Sigma) and the reaction mixture was dialyzed against distilled water for 2 days. Finally, the aqueous product solution was lyophilized and the desired product was isolated as a colorless solid. The chemical structure of the product was characterized via ^{1}H NMR spectroscopy. Yield: 31%–54%

TNBS Assay of PEI5K–PCL5K–PEI5K: To determine the PEI content in the copolymer PEI5K–PCL5K–PEI5K, a TNBS assay was carried out. TNBS is a rapid and sensitive assay reagent for the determination of free amino groups.[47] Primary amines, upon reaction with TNBS, form a highly chromogenic derivative, which has specific absorbance and can be used for quantitative measurements of amines.[48] A series of PEI5K high-purity water solutions were prepared as the standard solutions. An aliquot of 100 µL sample and the standard solution was mixed with 30 µL of a 1.76% TNBS solution (w/v in 0.1 M Borax) in a transparent microwell plate. After incubation at room temperature for 1 h, sample absorbance was assessed at 405 nm in a microplate reader (TECAN, Switzerland). Results were compared with the standard dilution series.

Preparation and Characterization of PEI–PCL–PEI/PEG–PCL Based Nanoparticles: The nanoparticles were prepared via solvent displacement method (nanoprecipitation) similar to method 1 described above. In brief, 200 µL PEI–PCL–PEI (5–5–5 kDa, 5 mg mL^{-1}) and 2, 4, or 8 µL of PEG–PCL (5–4 kDa, 5 mg mL^{-1}) in acetone was mixed and then injected into 1 mL distilled water while stirring (350 rpm). After stirring and evaporating the acetone in a fume hood for 3 h, the NPs in distilled water were characterized using a NanoZS zeta sizer (Malvern Instruments Inc., Malvern, UK).

For the preparation of siRNA-loaded nanoparticle–siRNA complexes (micelleplexes), the amounts of blank nanoparticles were calculated according to the following equation:

$$m\,(PEI-PCL-PEI)\;(inpg) = 50pmol \times 52 \times N/P \times 43.1gmol^{-1}/ 64.75\% \quad (2)$$

where 52 is the number of nucleotides of the 25/27mer siRNA; N/P ratio is the molar ratio of the polymer's protonale amine groups (N) and the siRNA phosphate groups (P); 43.1 g mol^{-1} is the protonable unit of PEI; 64.75% is the PEI amount in PEI–PCL–PEI determined by TNBS assay. The nanoparticle suspension was mixed with the siRNA solution and incubated at room temperature for 2 h to form micelleplexes ready to be used in subsequent experiments.

SYBR Gold Assay of PEI–PCL–PEI/PEG–PCL Based Nanoparticles: To determine the siRNA encapsulation efficiency of the nanoparticles, SYBR Gold assays were performed. In brief, the micelleplexes at N/P 1, 3, 5, 7, 10, 15, and 20 were prepared. In brief, 100 µL of the micelleplexes were added to a 96-well plate in triplicate. Free siRNA solution with the same amount of siRNA (N/P = 0) was used as negative control, and the fluorescence value was set as 100%. Subsequently, 30 µL of SYBR gold solution (4×) was added to the plate and incubated in the dark at room temperature for 10 min. Finally, the fluorescence was determined using a microplate reader (TECAN, Switzerland, excitation: 485/20 nm emission: 520/20 nm).

Dye Quenching Assay: Dye quenching of covalently modified molecules is another method to investigate the binding behavior of nucleic acids by polycations.[42] PEI–PCL–PEI NPs and PEI–PCL–PEI/PEG–PCL NPs were prepared as described above. Here, 30 pmol Cy5-siRNA was complexed with nanoparticles at different N/P ratios. The remaining fluorescence of the micelleplex suspensions (100 µL) was determined using a microplate reader (TECAN, Switzerland, excitation: 621/20 nm, emission: 666/20 nm). Free Cy5-siRNA in 10 mM HEPES buffer represents 100% fluorescence.

Cellular Uptake of PEI–PCL–PEI/PEG–PCL Based Nanoparticles: The nanoparticles were prepared as described above. Alexa Fluor 488 labeled siRNA (AF488-siRNA) was then incubated with the blank nanoparticles at room temperature for 2 h to form micelleplexes, and the cellular uptake was assessed by flow cytometry with a 488 nm laser for excitation and BL1 filter (530/30 nm) for detection.

GFP Knockdown of PEI–PCL–PEI/PEG–PCL Based Nanoparticles: The nanoparticles were prepared as described above. For nanoparticle loading, scrambled siRNA (siNC) or siRNA against GFP (siGFP) was incubated with the blank nanoparticles at room temperature for 2 h. H1299/eGFP cells were seeded in 24-well plate (25 000 cells in 500 µL medium per well), after growth in CO_2 incubator (37 °C, 5% CO_2) for 24 h, the cells were transfected with micelleplexes (NPs–siRNA complexes) composed of siNC (50 pmol per well) or siGFP (50 pmol per well). Lipofectamine 2000 formulated with siNC and siGFP were controlled groups. After 48 h in the incubator, the transfected cells were detached and washed with PBS for flow cytometry measurements (Attune Cytometer, Thermo Fisher Scientific, Darmstadt, Germany), with a 488 nm laser for excitation and BL1 filter (530/30 nm) for detection. To promote endosomal escape of the nanoparticles, chloroquine was incubated with the cells and polyplexes at a final concentration of 50 and 100 µM. Subsequently, the cells were analyzed as described above.

MTT Assay of PEI–PCL–PEI/PEG–PCL Based Nanoparticles: The PEI–PCL–PEI/PEG–PCL nanoparticles with different amount of PEG–PCL were diluted with complete RPMI-1640 medium to a concentration range from 2 to 100 µg mL^{-1}, and incubated with H1299 cells for 24 h. Hyperbranched PEI (25 kDa) was used as a control. The nanoparticle suspensions were then discarded, and MTT in serum-free RPMI-1640 medium (0.5 mg mL^{-1}) was incubated with the cells at 37 °C for 3 h. The MTT solution was subsequently replaced with DMSO and incubated at room temperature for 30 min. The absorbance was finally determined using a microplate reader (TECAN, Männedorf, Switzerland) at 570 nm and corrected with the background measurement at 680 nm.

Supporting Information

Supporting Information is available from the Wiley Online Library or from the author.

Acknowledgements

Y.J. appreciates the financial support from the China Scholarship Council (CSC201906010329). This project was funded by ERC-2014-StG—637830 to Olivia Merkel.

Open Access funding enabled and organized by Projekt DEAL.

Conflict of Interest

The authors declare no conflict of interest.

Data Availability Statement

The data that support the findings of this study are available from the corresponding author upon reasonable request.

Keywords

low molecular weight polyethylenimine, nanoprecipitation, polyethylene glycol-*b*-polycaprolactone, siRNA delivery

Received: September 28, 2022
Revised: November 17, 2022
Published online: December 9, 2022

[1] A. Fire, S. Xu, M. K. Montgomery, S. A. Kostas, S. E. Driver, C. C. Mello, *Nature* **1998**, *391*, 806.
[2] L. J. Scott, *Drugs* **2020**, *80*, 335.
[3] Y. Weng, H. Xiao, J. Zhang, X.-J. Liang, Y. Huang, *Biotechnol. Adv.* **2019**, *37*, 801.
[4] L. J. Scott, S. J. Keam, *Drugs* **2021**, *81*, 277.
[5] M. I. Sajid, M. Moazzam, S. Kato, K. Yeseom Cho, R. K. Tiwari, *Pharmaceuticals* **2020**, *13*, 294.
[6] Y. Liu, O. Samsonova, B. Sproat, O. Merkel, T. Kissel, *J. Controlled Release* **2011**, *153*, 262.
[7] W. Godbey, K. K. Wu, A. G. Mikos, *J. Biomed. Mater. Res.* **1999**, *45*, 268.
[8] D. Fischer, T. Bieber, Y. Li, H.-P. Elsässer, T. Kissel, *Pharm. Res.* **1999**, *16*, 1273.
[9] Y.-K. Oh, T. G. Park, *Adv. Drug Delivery Rev.* **2009**, *61*, 850.
[10] L. W. Seymour, R. Duncan, J. Strohalm, J. Kopeček, *J. Biomed. Mater. Res.* **1987**, *21*, 1341.
[11] M. A. Gosselin, W. Guo, R. J. Lee, *Bioconjugate Chem.* **2001**, *12*, 989.
[12] X. Ge, J. Feng, S. Chen, C. Zhang, Y. Ouyang, Z. Liu, W. Yuan, *J. Nanobiotechnol.* **2014**, *12*, 13.
[13] A. Ewe, S. Noske, M. Karimov, A. Aigner, *Pharmaceutics* **2019**, *11*, 600.
[14] A. Kichler, *J. Gene Med.* **2004**, *6*, S3.
[15] M. Karimov, D. Appelhans, A. Ewe, A. Aigner, *Eur. J. Pharm. Biopharm.* **2021**, *161*, 56.
[16] M. Zheng, Y. Zhong, F. Meng, R. Peng, Z. Zhong, *Mol. Pharmaceutics* **2011**, *8*, 2434.
[17] Z. Liu, Z. Zhang, C. Zhou, Y. Jiao, *Prog. Polym. Sci.* **2010**, *35*, 1144.
[18] V. Incani, A. Lavasanifar, H. Uludağ, *Soft Matter* **2010**, *6*, 2124.
[19] X. Shuai, T. Merdan, F. Unger, M. Wittmar, T. Kissel, *Macromolecules* **2003**, *36*, 5751.
[20] Y. Liu, J. Nguyen, T. Steele, O. Merkel, T. Kissel, *Polymer* **2009**, *50*, 3895.
[21] T. Endres, M. Zheng, A. Kilic, A. Turowska, M. Beck-Broichsitter, H. Renz, O. M. Merkel, T. Kissel, *Mol. Pharmaceutics* **2014**, *11*, 1273.
[22] V. Mosqueira, P. Legrand, R. Gref, B. Heurtault, M. Appel, G. Barratt, *J. Drug Targeting* **1999**, *7*, 65.
[23] C. E. Mora-Huertas, H. Fessi, A. Elaissari, *Adv. Colloid Interface Sci.* **2011**, *163*, 90.
[24] S. A. Vitale, J. L. Katz, *Langmuir* **2003**, *19*, 4105.
[25] F. Ganachaud, J. L. Katz, *ChemPhysChem* **2005**, *6*, 209.
[26] M. Chacón, L. Berges, J. Molpeceres, M. R. Aberturas, M. Guzman, *Int. J. Pharm.* **1996**, *141*, 81.
[27] N. Anarjan, N. Jaberi, S. Yeganeh-Zare, E. Banafshehchin, A. Rahimirad, H. Jafarizadeh-Malmiri, *J. Am. Oil Chem. Soc.* **2014**, *91*, 1397.
[28] W. S. Saad, R. K. Prud'homme, *Nano Today* **2016**, *11*, 212.
[29] S. A. Guhagarkar, V. C. Malshe, P. V. Devarajan, *AAPS PharmSciTech* **2009**, *10*, 935.
[30] T. Ameller, V. Marsaud, P. Legrand, R. Gref, J.-M. Renoir, *Eur. J. Pharm. Sci.* **2004**, *21*, 361.
[31] M. Beck-Broichsitter, E. Rytting, T. Lebhardt, X. Wang, T. Kissel, *Eur. J. Pharm. Sci.* **2010**, *41*, 244.
[32] S. M. Moghimi, A. C. Hunter, J. C. Murray, *Pharmacol. Rev.* **2001**, *53*, 283.
[33] M. Elsayed, V. Corrand, V. Kolhatkar, Y. Xie, N. H. Kim, R. Kolhatkar, O. M. Merkel, *Biomacromolecules* **2014**, *15*, 1299.
[34] S. Kly, L. J. Andrew, E. G. Moloney, Y. Huang, J. E. Wulff, M. G. Moffitt, *Chem. Mater.* **2021**, *33*, 6860.
[35] V. Izumrudov, T. K. Bronich, M. Novikova, A. Zezin, V. Kabanov, *Polym. Sci.* **1982**, *24*, 367.
[36] A.-L. Bolcato-Bellemin, M.-E. Bonnet, G. Creusat, P. Erbacher, J.-P. Behr, *Proc. Natl. Acad. Sci. U. S. A.* **2007**, *104*, 16050.
[37] O. M. Merkel, D. Librizzi, A. Pfestroff, T. Schurrat, K. Buyens, N. N. Sanders, S. C. De Smedt, M. Béhé, T. Kissel, *J. Controlled Release* **2009**, *138*, 148.
[38] N. Hartl, F. Adams, G. Costabile, L. Isert, M. Doblinger, X. Xiao, R. Liu, O. M. Merkel, *Nanomaterials* **2019**, *9*, 986.
[39] T. F. Martens, K. Remaut, J. Demeester, S. C. De Smedt, K. Braeckmans, *Nano Today* **2014**, *9*, 344.
[40] J. Dolai, K. Mandal, N. R. Jana, *ACS Appl. Nano Mater.* **2021**, *4*, 6471.
[41] L. Jamalzadeh, H. Ghafoori, R. Sariri, H. Rabuti, J. Nasirzade, H. Hasani, M. R. Aghamaali, *Avicenna J. Med. Biochem.* **2016**, *4*, 10.
[42] M. Zheng, G. M. Pavan, M. Neeb, A. K. Schaper, A. Danani, G. Klebe, O. M. Merkel, T. Kissel, *ACS Nano* **2012**, *6*, 9447.
[43] A. Santel, M. Aleku, O. Keil, J. Endruschat, V. Esche, G. Fisch, S. Dames, K. Löffler, M. Fechtner, W. Arnold, K. Giese, A. Klippel, J. Kaufmann, *Gene Ther.* **2006**, *13*, 1222.
[44] M. Dominska, D. M. Dykxhoorn, *J. Cell Sci.* **2010**, *123*, 1183.
[45] D. T. Wiley, P. Webster, A. Gale, M. E. Davis, *Proc. Natl. Acad. Sci. U. S. A.* **2013**, *110*, 8662.
[46] Y. Jin, Q. Liu, C. Zhou, X. Hu, L. Wang, S. Han, Y. Zhou, Y. Liu, *Nanoscale* **2019**.
[47] A. S. A. Habeeb, *Anal. Biochem.* **1966**, *14*, 328.
[48] G. T. Hermanson, *Bioconjugate Techniques*, 3rd ed., Academic Press, Cambridge, MA **2013**.